Journal of New Materials for Electrochemical Systems 19, 27-32 (2016)

Sol-gel Synthesis and Characterizations of $MgSO_4$- Al_2O_3 Composite Solid Electrolytes

N. Che Su[1,*], M. Sulaiman[2,†] and N.S. Mohamed[2,‡]

[1]Institute of Graduate Studies, University of Malaya 50603 Kuala Lumpur, Malaysia
[2]Center for Foundation Studies in Science, University of Malaya 50603 Kuala Lumpur, Malaysia

Received: January 06, 2016, Accepted: March 17, 2016, Available online: April 29, 2016

Abstract: *In this study, composite solid electrolytes in the system (1-x) $MgSO_4$ – x Al_2O_3 with x = 0.1 - 0.6 mole were prepared by a citric acid assisted sol-gel method. X-ray diffraction analysis confirmed the transformation of anhydrous $MgSO_4$ to β-$MgSO_4$ upon sintering at 900 ˚C for 2 hours. The prepared composite samples exhibited both crystalline and amorphous state of β-$MgSO_4$. The highest conductivity found was 1.9 ×10^{-6} S cm^{-1} with x = 0.6 at elevated temperatures. The current results show that high concentration of Al_2O_3 enhanced the disordered phase composite sample thus contributes to high concentration amorphous of composite samples. This has been supported by FTIR, DSC and SEM.*

Keywords: Composite solid electrolyte, magnesium sulphate, aluminium oxide, sol-gel method

1. INTRODUCTION

The field of superionic solids has been considered as one of the major thrust area of research due to the exciting technological relevance of this material in developing wide variety of all solid-state electrochemical devices such as batteries, gas separation membranes, chemical sensors and ion switches. Another reason for the researchers to look for solids with high ion conduction at room temperature is the disadvantages of liquid electrolytes. The use of solid electrolytes can avoid problems related to liquid electrolytes such as limited range of temperatures, electrode corrosion by electrolytic corrosion and subject to leakage [1].

Among the many solid electrolytes available, composite solid electrolytes are among of the potential solid electrolytes which not only offer high ionic conductivity but also better mechanical properties. Besides that, composite solid electrolytes with appreciably high ionic and negligible electronic conductivity are attractive materials for solid-state batteries and sensors. Conductivity of composites is governed mainly by the ionic transport via interface regions of the ionic crystals. The specific interface interactions between the components lead to the stabilization of strongly disordered states of ionic components at the interface such as amorphous. Prior literature lithium-based solid electrolytes were successfully prepared and showed high conductivity values [2]. However, high reactivity of lithium metal resulted in difficulty in handling as they need to be prepared in a nitrogen glove box. Hence, there are many research efforts currently pursued to develop and characterized Mg-ion conducting solid electrolyte material due to being eco-friendly, non-toxic and abundant in nature compared to lithium material [3]. Various procedures have been applied to increase the conductivity of composite solid electrolytes. One of the most successful methods used to prepare the composite samples is sol-gel method [4, 5]. This method offers many advantages over conventional method such as low synthesis temperature, high homogeneity and ability to shape the products into various forms [1, 6]. $MgSO_4$ salt is one of the safest and edible magnesium salts that can conduct Mg^{2+} ion. However, this type of salt possesses a low conductivity due to strong electrostatic forces between Mg^{2+} and SO_4^{2-} ions. The main challenge to resolve is to increase it conductivity. Subsequent to Liang's discovery, the dispersion of alumina particles into to the host material enhanced the charge carrier concentration in the space charge region near the interface between the electrolyte matrix and dispersoids thus increasing the conductivity [2].

In this light, we appraised the conductivity of $MgSO_4$- Al_2O_3 composite solid electrolytes via a sol-gel method. We further evaluated the structural properties and conductivity mechanism of magnesium sulphate: aluminium oxide composite system with the additional support to the formation of disorientation of β- $MgSO_4$

To whom correspondence should be addressed:
Email: *ahaslincs@gmail.com, †mazdidas@um.edu.my, ‡nsabirin@um.edu.my

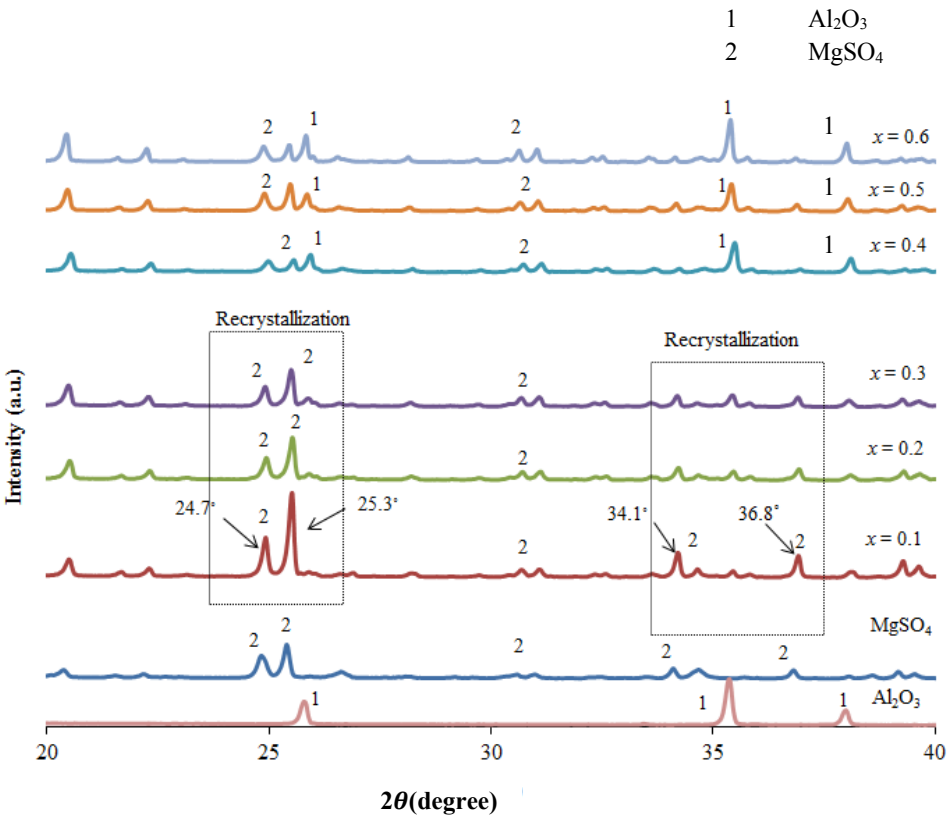

Figure 1. XRD pattern of anhydrous $MgSO_4$, Al_2O_3 and (1-x) $MgSO_4$ – x Al_2O_3 with x = 0.1 - 0.6 composite samples.

crystal structure. Next, X-ray diffraction (XRD), Fourier transform infrared (FTIR), scanning electron microscopy (SEM), and impedance spectroscopy were employed to examine the structural, thermal, electrical and electrochemical studies of the composite system which applicable in composite solid rechargeable batteries.

2. EXPERIMENTAL

2.1. Sample Preparation

In this study, analytical grade anhydrous $MgSO_4$ and Al_2O_3 from Sigma Aldrich were used as starting materials. Desired amount of $MgSO_4$ from the formula (1-x) $MgSO_4$: x Al_2O_3 with x = 0.1-0.6 was dissolved in ethanol under magnetic stirring at room temperature. The calculations involved in preparation process are as follows:

For example: x = 0.1 mol of Al_2O_3

Mass used = 0.1 × 101.96 g mol^{-1} (molar mass of Al_2O_3)

A required mole of Al_2O_3 was then added into the initial solution. Citric acid with equivalent amount to the Al_2O_3 was also added into the solution and a gel was formed after refluxing on a hot plate for 24 h at 80 °C. The gel formed was then dried at 200 °C for 5 h in a drying oven followed by sintering process at 900 °C for 2 h. The final product obtained was a voluminous, fluffy, and white powder. The powder was later crushed in an agate mortar into 25 nm powder.

2.2. Sample Characterization

Structural characteristics of the samples were obtained using X-ray diffraction spectrometer. In this study, the XRD patterns of composite samples were taken using D8 Advanced X-ray Diffractometer-Buker AXS with Cu-K_α radiation of wavelength1.5406°. The 2θ ranged from 10º to 40º and was 0.026º. Thermal analyses were performed with a Setaram Labsys Evo TG-DTA/DSC equipment in the temperature range from 30°C to 1200 °C. FTIR was carried out to confirm the structure of the studied composite samples. Infrared spectra were recorded at room temperature using a Perkin Elmer Frontier Spectrometer with 2 cm^{-1} resolution. The spectral data were collected in the spectral range from 550-1400 cm^{-1} and used to identify the presence of the materials phases of the composite. The analysis revealed any transformation occurred in the composites. Next, the morphology of cross section images of the sample and chemical content of the composite were studied by using Zeiss Evo MA10 Scanning Electron Microscopy. The composite electrical properties were determined by impedance spectroscopy using a Solartron 1260 impedance analyzer over the frequency range from 0.1 to 10^6 Hz. The applied voltage was set at 200 mV and all the measurement were taken at temperatures of between 30 and 200 ºC . The conductivity was calculated by using the equation:

$$\sigma_b = \frac{t}{R_b A}$$

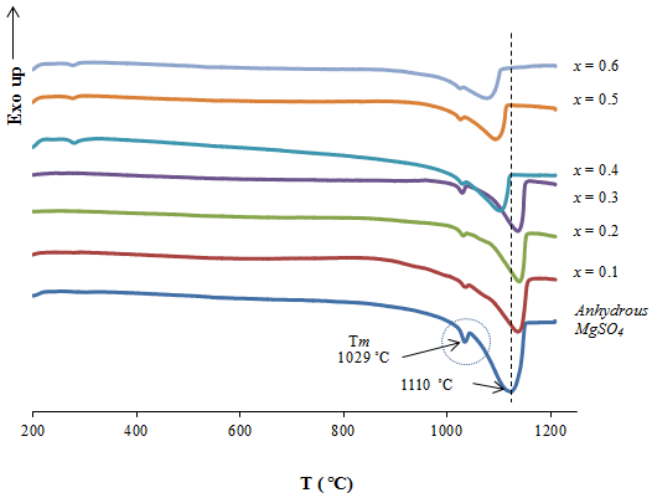

Figure 2. DSC curves for anhydrous $MgSO_4$ and composite samples of x = 0.1-0.6

where, t is the thickness of the samples, A is the cross-sectional area of the electrode with diameter of 13 mm and R_b is the bulk resistance with thickness. The average the thickness is 0.48 mm.

3. RESULTS AND DISCUSSION

3.1. XRD analysis

Fig. 1 shows XRD spectra of anhydrous $MgSO_4$, Al_2O_3 and the prepared composite samples with x = 0.1-0.6. The XRD pattern of anhydrous $MgSO_4$ shows crystalline characteristics with predominant peaks at 2θ = 24.7˚, 25.3˚, 34.1˚ and 36.8˚. A similar observation was reported [7]. The XRD spectra of the composite samples shows the characteristics peak of Al_2O_3 at 2θ = 25.7°, 35.3° and 37.9°. This confirms the composite nature of the composite samples with x = 0.1- 0.6 [8].

From the spectra, it was identified that all composite samples were transformed into β-$MgSO_4$ phase in correspondence with standard β-$MgSO_4$ powder data (reference code 98-002-7130). The possible pathway of phase transition of $MgSO_4$ can be represented by the following route:

$$\text{Anhydrous } MgSO_4 \xrightarrow[900^oC]{} \beta\text{ - } MgSO_4$$

A close examination shows that with the addition of Al_2O_3 of x = 0.1-0.3, the peak intensity of $MgSO_4$ at 2θ = 24.7˚, 25.3˚, 34.1˚ and 36.7˚ increased and become narrowed compared with anhydrous $MgSO_4$. This corresponds to the recrystallization phase of $MgSO_4$ crystallite phase in the composite samples due to sintering process at 900 ˚C during preparation. However the intensity of these peaks were decreased with the addition of alumina of x = 0.4-0.6. The broadening and the disappearance of the peaks suggest the formation of amorphous phase in the composite samples [9]. This phase was expected to form at the $MgSO_4$-Al_2O_3 interface as a result of chemical and physical interactions of $MgSO_4$ and Al_2O_3 phases. In general, all composite samples consists both amorphous and crystalline states of β - $MgSO_4$.

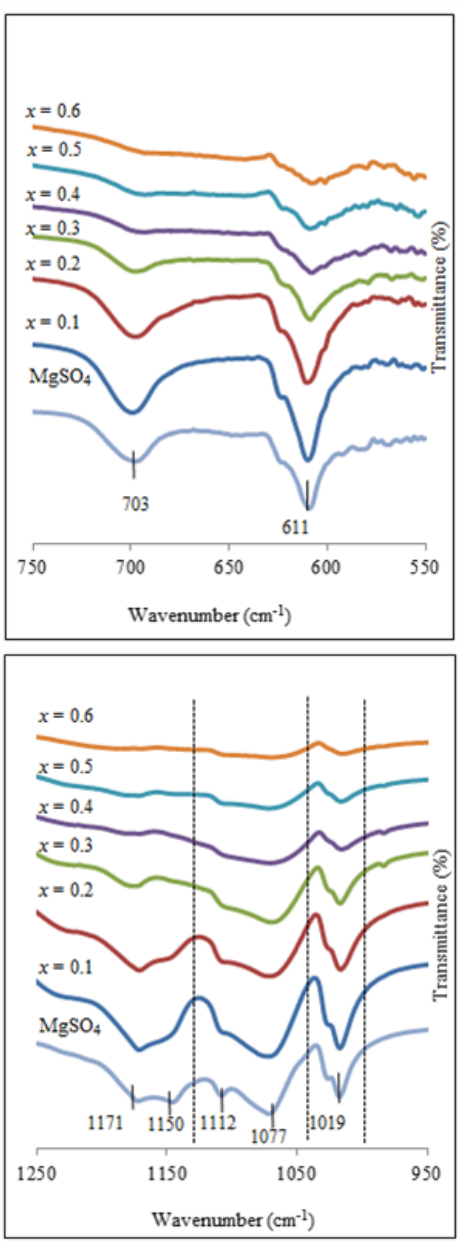

Figure 3. FTIR spectra of anhydrous $MgSO_4$ and the prepared composite samples

3.2. DSC analysis

Fig. 2 depicts the DSC curves for $MgSO_4$ and composites with x = 0.1-0.6 in the temperature range of 200-1200 ˚C. A stable phase of $MgSO_4$ and all composite samples appeared between 200 ˚C and 1029 ˚C.

According to literature [10-11], anhydrous magnesium sulphate co-exists as polymorph of α-$MgSO_4$ and β-$MgSO_4$ at temperature below than ~527 ˚C. However, with continuous heating of α-$MgSO_4$ higher than 595 ˚C, the fully formation of β-$MgSO_4$ had occurred .The possible pathway of phase transformation occurred as follows:

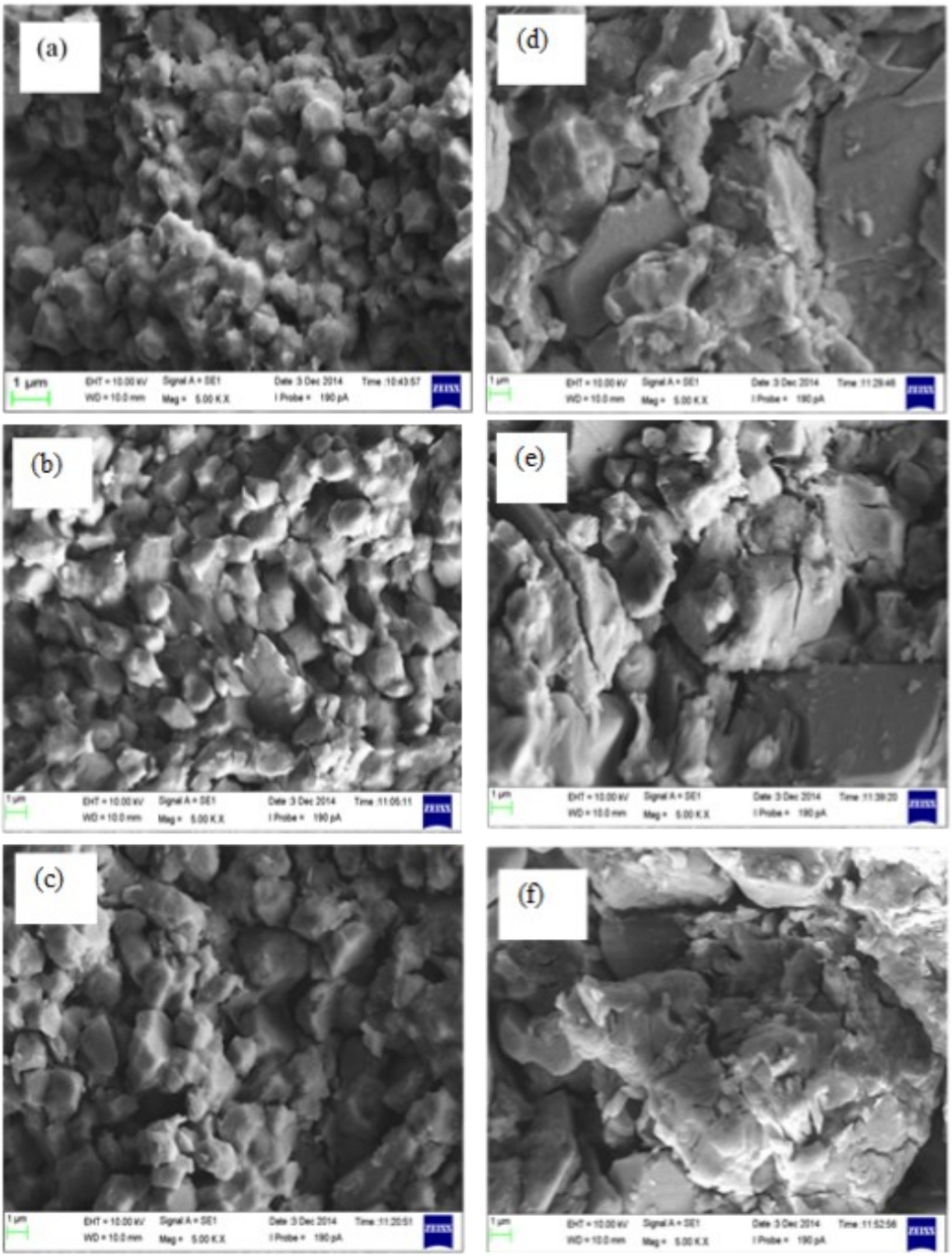

Figure 4. Morphology of composite samples with (a) x = 0.1, (b) x = 0.2, (c) x = 0.3, (d) x = 0.4, (e) x = 0.5 and (f) x = 0.6

$$\text{Anhydrous } MgSO_4 \xrightarrow[\sim 527\ ^{o}C]{} \alpha\text{ - }MgSO_4 \xrightarrow[\sim 595\ ^{o}C]{} \beta\text{ - }MgSO_4$$

Two endothermic peaks were identified in the curve for anhydrous $MgSO_4$ compound. The endothermic peak peaks at 1029 ˚C correspond to melting point while 1110 ˚C and decomposition of the compound respectively. The decomposition phase of the composite sample with x = 0.1-0.3, is shifted to higher temperature. This support the recrystallization phase as discussed in XRD. However, with the addition of alumina, the decomposition band for samples x = 0.4-0.6, had shifted to lower temperature. This suggests the formation of high amorphous of β-$MgSO_4$ with the addition of alumina [10].

Moreover, an endothermic peak at 1029 ˚C corresponds to incongruent melting of β-$MgSO_4$ phases. It should be noted that, with the addition of alumina, the composite sample with x= 0.4-0.6 showed

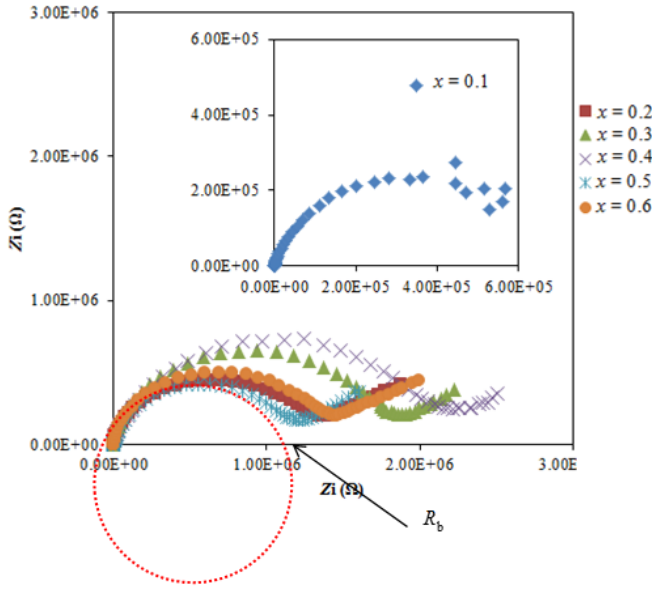

Figure 5. Cole-cole plot of composite samples with x = 0.1 – 0.6 at room temperature.

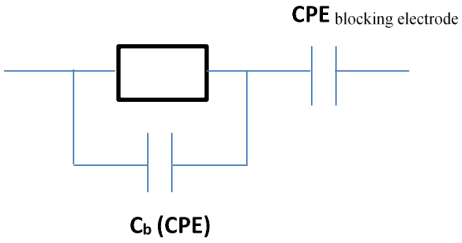

Figure 6. Electrical equivalent circuit of the composite sample based on impedance analysis of the samples at room temperature.

less intense peak compared with x =0.1-0.3. This implies the transformation of β-$MgSO_4$ to both crystalline and amorphous state. A similar effect was observed previously in other system of the ionic salt-oxide type [11, 12].

3.3. FTIR analysis

Fig. 3 shows the FTIR spectra of anhydrous $MgSO_4$ and the prepared composite samples (x = 0.1-0.6). The spectrum of $MgSO_4$ shows strong absorption band at 611, 703, 1019, 1077, 1112, 1150 and 1171 cm^{-1} [13]. These characteristics of sulphate group were also observed in all composites samples. This suggests the presence of $MgSO_4$ in all composite samples. In addition, it has been reported that the band absorption of the sulfate ion appeared at 613 cm^{-1}.

However, the intensity of the peak decreases with increase of alumina which probably resulted from the combined absorptions of sulphate with the dispersoid [14]. In this study, addition of alumina into the composite samples the absorption bands S-O stretching at 1077-1112 and 1150- 1171 cm^{-1} overlapped to become one wide peaks results which indicate that the effect of alumina on the β-$MgSO_4$.

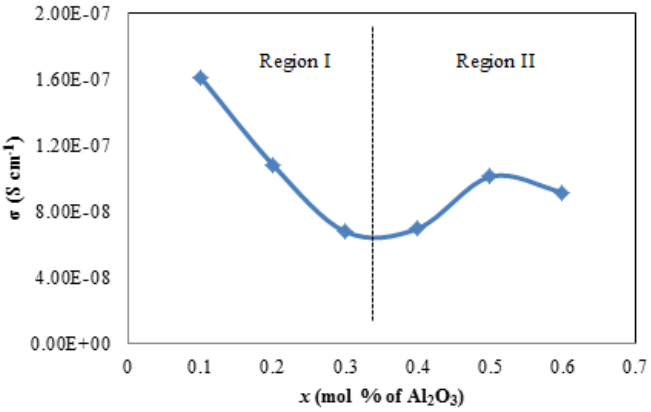

Figure 7. Ionic conductivity as a function of composition (x) for $MgSO_4$-Al_2O_3 composite samples at room temperature

3.4. SEM/ EDX Analysis

Fig. 4 shows the cross-sectional SEM micrograph of the composite samples compositions of x = 0.1-0.6. The composite samples with x = 0.1-0.3 were dominanted with crystalline phase of β-$MgSO_4$ while high amorphous phase were observed in composite samples with x = 0.4-0.6. The crystalline phase of β-$MgSO_4$ in composite sample x = 0.1-0.3 were due the recrystallization as dicussed in previous section. This feature could impede the conducitivty behaviour of the composite samples as it leads to poor contact between the crystalline β-$MgSO_4$ and alumina [7,8]. On the other hand, composite samples with x = 0.4-0.6 showed β-$MgSO_4$ appeared in both crystalline and amorphous which created contact between the β-$MgSO_4$ and alumina.

3.5. Electrical conductivity

The Cole-Cole plots of composite samples with x = 0.1 – 0.6 are depicted in Fig. 5. They consist of one electrode spike region. The high frequency the semicircle is assigned to the bulk response with its intercept at the x-axis assigned to bulk resistance (R_b). Meanwhile, Fig. 6 shows that the complex impedance data obtained experimentally for the composite samples may be denoted by the impedance of an equivalent circuit comprised of bulk resistance (R_b) and a blocking electrode with constant phase element (CPE) [15].

In addition, Fig. 7 shows that there are two types of conductivity mechanism occurred in the prepared composite system. For the first part of the plot (region I), the conductivity decreased from x = 0.1 to 0.3. The decreased of conductivity is due to the recrystallization of β-$MgSO_4$ during sintering. Nevertheless, the conductivity composite samples with x = 0.4 to 0.5 increase. This suggests that amorphous phase helps the whole volume of ionic salts to get into the interface region [16, 17]. However, the addition of more Al_2O_3 in composite sample with x=0.6 results in decrease of the conductivity. This may due to the agglomerations of alumina particles which hinder the motion of mobile ions [18].

Fig. 8 illustrates the temperature dependence of conductivity for the compos ite samples in the system (1-x) $MgSO_4$ – x Al_2O_3. It showed that the conductivity value of the composite system increased gradually from room temperature to 200 ºC with tempera-

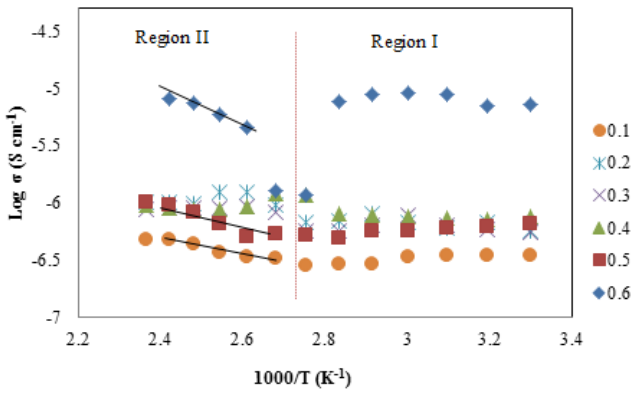

Figure 8. The ionic conductivity of $MgSO_4$-Al_2O_3 composite samples versus inverse of temperature at various compositions

ture. All the composites sample were thermally activated due to thermal vibrations which caused the ion to receive enough energy to be pushed into interstitial sites or to nearby vacant lattice site, that leads to ion conduction [18, 19]. Two conductivity changes occur in the system at temperature range from 30-90 (region I) and from 100 to 150 (region II). In general, low conductivity was caused by the effect of continuous "freezing" of cations at the interface of magnesium and alumina [9]. The high concentration of amorphous phase in the composite samples was due to increase in temperature ensuring high conductivity in region II.

4. CONCLUSION

Composite solid electrolytes of (1-*x*) $MgSO_4$- *x* Al_2O_3 have been successfully prepared using a sol-gel method. The XRD pattern revealed that the prepared composite samples consisted of crystalline and high concentration of amorphous phase of β-$MgSO_4$. The presence of these phases was further confirmed by DSC, FTIR and SEM results. DSC analysis revealed that the addition of alumina has lowered the melting points of the composite samples. The high ionic conductivities of the prepared composite samples were due to the presence of high concentration of amorphous phase of β-$MgSO_4$.

5. ACKNOWLEDGEMENT

The author would like to that the University Malaya for providing the UMRG (RG254-13AFR) and PPP (PG-095-2014A) research grant to support this work.

REFERENCES

[1] Kumar, B., Nellutla, S., Thokchom, J. S., & Chen, C., Journal of power sources, 160, 1329 (2006).
[2] Liang C.C., Journal of the Electrochemical Society, 120, 1289 (1973).
[3] Ahmad A.H. & Ghani F.S., American Institute of Physics Conference Series, 1136, 31 (2009).
[4] Dzulkurnain N.A. & Mohamed N.S., Advanced Materials Research, 129, 506 (2010).
[5] Mat H., Mohamed N.S. & Subban R.H.Y., Advanced Materials Research, 415, 442 (2011).
[6] Yoshimoto N., Yakushiji S., Ishikawa M. & Morita M., Electrochimica acta, 48, 2317 (2033).
[7] Manam J. & Das S., Solid State Sciences, 12(8), 1435 (2010).
[8] Sulaiman M., Rahman A.A. & Mohamed N.S., Int. J. Electrochem. Sci, 8, 6647 (2013).
[9] Uvarov N.F., Journal of Solid State Electrochemistry, 15, 367 (2011).
[10] Rao M.M., Reddy S.N. & Chary A.S., Physica B: Condensed Matter, 389, 292 (2007).
[11] Fortes A.D., Wood I.G., Vočadlo L., Brand H.E.A. & Knight K.S., Journal of Applied Crystallography, 40, 761 (2007).
[12] Scheidema M.N. & Taskinen P., Industrial & Engineering Chemistry Research, 50, 9550 (2011).
[13] Smith D.H. & Seshadri K.S., Spectrochimica Acta Part A: Molecular and Biomolecular Spectroscopy, 55, 795 (1999).
[14] Ovalles F., Gallignani M., Rondón R., Brunetto M.R. & Luna R., Lat. Am. J. Pharm, 28, 173 (2009).
[15] Kubanska A., Castro L., Tortet L., Schäf O., Dollé M. & Bouchet R., Solid State Ionics, 266, 44 (2014).
[16] Sulaiman M., Dzulkarnain N.A., Rahman A.A. & Mohamed N.S., Solid State Sciences, 14, 127 (2014).
[17] Sultana S. & Rafiuddin R., Ionics, 155, 621 (2009).
[18] Agrawal R.C., Verma M.L. & Gupta R.K., Solid State Ionics, 171, 199 (2004).
[19] Agrawal R.C. & Gupta R.K., Journal of materials science, 34, 1131 (1999).